



## Aging of large-area CsI photocathodes for the ALICE HMPID prototypes

A. Braem<sup>a</sup>, M. Davenport<sup>a</sup>, A. Di Mauro<sup>a</sup>, P. Martinengo<sup>a</sup>,  
E. Nappi<sup>b</sup>, G. Paic<sup>a</sup>, F. Piuz<sup>a</sup>, E. Schyns<sup>a</sup>

<sup>a</sup>*CERN, Geneva, Switzerland*

<sup>b</sup>*INFN- Sez. di Bari, Bari, Italy*

Presented by A. Di Mauro

**Elsevier use only:** Received date here; revised date here; accepted date here

---

### Abstract

The ALICE HMPID RICH detector is equipped with CsI photocathodes in a MWPC for the detection of Cherenkov photons. The long-term operational experience with large-area CsI photocathodes is described. The RICH prototypes have shown a very high stability of operation and performance at a gain of  $10^5$  and with rates up to  $2 \times 10^4 \text{ cm}^{-2} \text{ s}^{-1}$ . When exposure to air is avoided, no degradation of the CsI quantum efficiency has been observed on photocathodes periodically exposed to test-beams over 7 years, corresponding to local integrated charge densities of  $\sim 1 \text{ mC cm}^{-2}$ . The results of limited exposures to oxygen and humidity are also presented.

© 2001 Elsevier Science. All rights reserved

*Keywords:* CsI, photocathode aging, RICH

### 1. Introduction

ALICE is the only LHC experiment dedicated to heavy ion physics [1]; it will study p-p, p-A and A-A collisions at a center of mass energy  $\sqrt{s} = 5.5 \text{ A TeV}$ . The ALICE High Momentum Particle IDentification (HMPID) system is based on a RICH detector equipped with CsI photocathodes (PCs) for the

detection of the Cherenkov light [2]. In Pb-Pb collisions, at the highest predicted multiplicity  $dN_{ch}/dy \sim 8000$ , 100 charged particles per  $\text{m}^2$  are expected to cross the HMPID detector, located 5 m from the vertex, with an interaction rate of 8 kHz.

Several groups have investigated CsI thin-film aging in the last years, however, it is neither well quantified nor fully understood. The basic processes and a collection of data are reviewed in [2,3,4,5]. The quantum efficiency (QE) of a CsI PC may degrade

due to modifications of the crystal lattice structure and stoichiometry. CsI and the single elements Cs and I react rapidly with water; Cs also easily oxidizes [6]. Since any exposure to air has to be avoided, the handling and the mounting on a detector may be difficult, especially with large PCs ( $\sim 50 \times 50 \text{ cm}^2$ ). QE degradation can also be generated by the impact of the avalanche ions, when the PCs are operated in a gaseous detector, or by the photon flux only (without charge multiplication). Other degradation sources may be the contamination of the surface by impurities (which will not be treated in this paper) and the radiation damages by neutral or charged particles. Usually, aging studies are carried out on small CsI samples through accelerated tests reaching, in a few weeks or months, integrated charges comparable to several years of operation in the anticipated environment of the experiment. In this paper, we will describe our long-term experience with large-area CsI PCs, periodically exposed to test-beams and also used in the STAR experiment at BNL. The results of exposures to high levels of oxygen or water vapour will also be presented.

## 2. Detector description and PC characteristics

Fig. 1 shows the principle scheme of the CsI-RICH detector; a detailed description can be found in [2,7]. The HMPID RICH has a proximity focusing geometry; the radiator, 15 mm thick, is liquid  $\text{C}_6\text{F}_{14}$  contained in a Neoceram<sup>®</sup> tray with a 5 mm fused silica exit window to transmit the UV Cherenkov photons. The photon detector is a MWPC with 4 mm sensitive gap, 20  $\mu\text{m}$  anode wires with 4.2 mm pitch. It is operated with  $\text{CH}_4$  at atmospheric pressure and has a pad cathode covered with a 300 nm photosensitive layer of CsI. The proximity gap (the gap between the quartz window and the pad plane) measures 80 mm.

Within the CERN project RD26, 32 CsI PCs, with areas from  $20 \times 10$  to  $64 \times 40 \text{ cm}^2$ , have been produced in the period 1993-1997 [8]. This project, aiming at the study of photosensitive CsI films for the detection of Cherenkov light, allowed the definition of a procedure to prepare large area CsI PCs with reproducible high QE. Fig.2 presents the QE at 170 nm for the produced PCs, including the last five

recently produced in the framework of the HMPID project. The improvement observed with PC19 was due to a new substrate preparation (Cu-clad PCB coated with Ni/Au layers and polished), the heat treatment, and the use of a dedicated transfer system

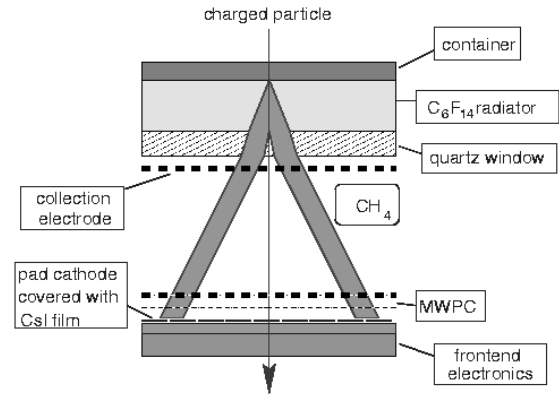


Fig. 1 Schematic view of the proximity focusing CsI-RICH detector. The lateral section of the cone represents the emitted Cherenkov light.

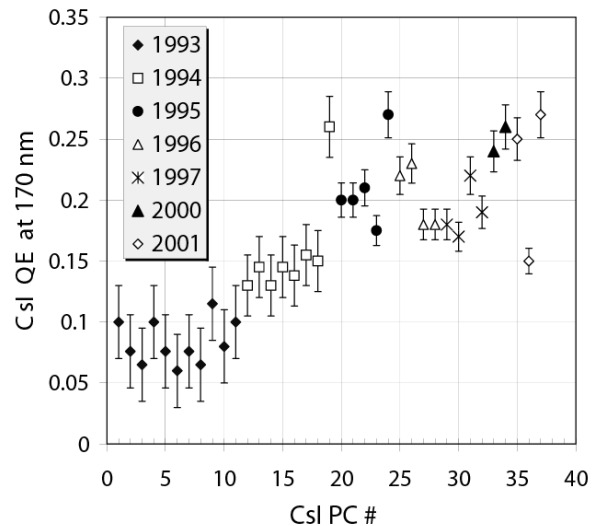


Fig. 2 Overview of the QE measured at 170 nm of the CsI PCs produced for the HMPID detector prototypes

for the detector assembly to avoid exposure to air [2,9].

The PCs selected for this study are: PC19, PC24, PC29, PC30, PC31, and PC32. PC19 and PC24 were produced in November 1994 and December 1995, respectively. They measure  $30 \times 32 \text{ cm}^2$  and are used in the HMPID RICH proto-1. PC29 to PC32 have an area of  $40 \times 64 \text{ cm}^2$  and were produced during June and July 1997. They are part of the larger proto-2, measuring 2/3 of a full HMPID module that is equipped with six PCs. At the end of 1999, proto-2 was installed in the STAR experiment at BNL.

### 3. QE extraction from test-beam data

The QE of the PCs is deduced from test-beam data with a procedure fully described in [10] and based on the comparison between experimental results and Monte Carlo simulation of Cherenkov events. Series of runs are taken, varying the high voltage on the anode wires and (only with proto-1) the radiator thickness or the proximity gap. The main steps of the analysis are:

- definition of a fiducial area which includes all Cherenkov photons that reach the PC, depending on the detector geometry and the beam momentum (Fig. 3);
- pad-cluster analysis and deconvolution, to locate single photoelectron clusters and measure the chamber gain (single-electron mean pulse height);
- evaluation of the main quantities: cluster multiplicity and size, total pad hits, ring radius spread, and Cherenkov angle resolution;
- tuning of a CsI QE curve with a Monte Carlo detector simulation, where all the processes, from the Cherenkov photons generation up to the signal induced on the pads, are taken into account.

Fig. 4 shows the differential QE of PC19, measured in different test-beams over a period of 7 years.

### 4. Operational experience with CsI PCs

After coating with CsI, a first performance evaluation is carried out in a test-beam. Then, the

PCs are kept in storage boxes under Ar flow and re-evaluated periodically to monitor their stability, typically with one week of irradiation at test-beams of the RICH prototypes. For each PC, a large collection of data has been reviewed to point out the correlation between any observed QE decrease and the possible contact with aging sources .

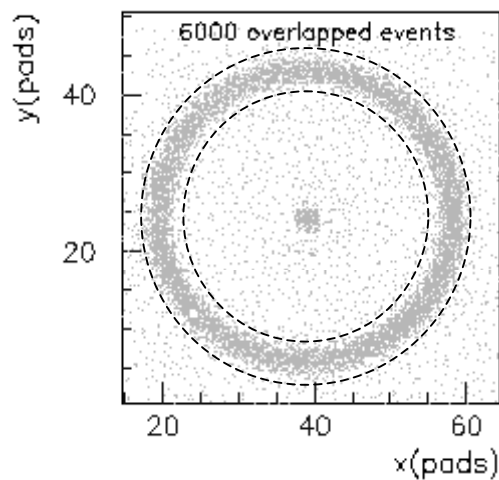


Fig. 3 Pad hits produced by 6000 overlapped Cherenkov events generated by 350 GeV/c pions, with 10 mm of  $\text{C}_6\text{F}_{14}$  and a proximity gap of 100 mm. The pad size is  $8 \times 8 \text{ mm}^2$ . The dashed lines delimit the fiducial area of the Cherenkov photons, while the spot in the center corresponds to the particles traversing the detector in a  $1 \text{ cm}^2$  area as defined by the event trigger scintillators.

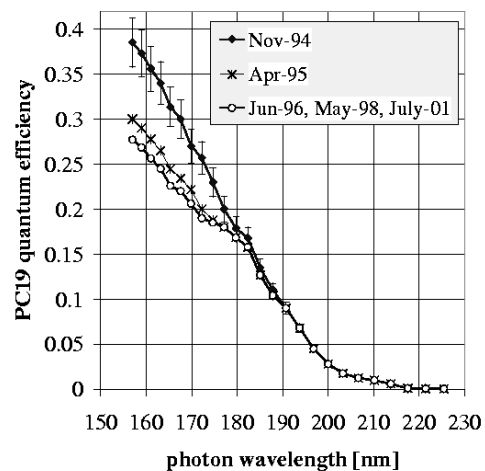


Fig. 4 PC19 differential QE, from the production date, Nov-94, until July-01, extracted from test-beam data. The degradation observed after the production was due to exposure to air.

#### 4.1. Detector aging

It is worth to mention that all the HMPID RICH prototypes are made out of aluminum frames and were assembled using standard construction materials (e.g. G10, Araldite AW106, Viton o-rings). During several years of use, under a gas gain of  $10^5$  and irradiation rates of  $\sim 10^4 \text{ cm}^{-2} \text{ s}^{-1}$ , no symptoms of detector aging (gain loss, Malter effect, discharges) have been observed.

#### 4.2. PC aging

The experimental conditions have to be considered in order to estimate the contribution of the different aging sources: the exposure to  $\text{O}_2$  and  $\text{H}_2\text{O}$ , the accumulated charge density corresponding to ion impact, and the total integrated photon flux.

##### i) Exposure to $\text{O}_2$ and $\text{H}_2\text{O}$

After coating with CsI, the PC is transferred into a protective storage box without any exposure to air and kept constantly under Ar flow (10-20 l/h) at  $\text{O}_2$  and  $\text{H}_2\text{O}$  levels lower than 10 ppm. At each test-beam, mounting and dismounting on the detector are executed inside a glove box, with an exposure for about 1 h to 400 ppm of  $\text{O}_2$  and 100 ppm of  $\text{H}_2\text{O}$ . Only PC19, for which such a glove box was not yet available, experienced three assembly operations in air, under relative humidity of 50%. During the beam test, the concentration of contaminants is generally lower than 10 ppm.

Dedicated tests were also carried out with high levels of  $\text{O}_2$  and  $\text{H}_2\text{O}$ , in stagnant conditions or under gas flow [11]. The PCs were checked in a test-beam before and soon after the exposures and no change in the QE has been noticed. The results of this study have been used to plan the shipment of the four PCs, PC29 to PC32 by aircraft, for the installation of proto-2 in the STAR experiment at BNL. During the shipment the PCs were kept inside sealed vessels pressurized with Ar at 1.2 bar.

##### ii) Ion impact.

To evaluate the accumulated charge density, one has to distinguish between avalanches produced by charged particles and those generated by single photoelectrons.

a) *PC19 and PC24* - These PCs, mounted on proto-1, were irradiated always with the beam crossing the detector in the center (Fig. 3). In this case, the area illuminated by the Cherenkov radiation is fixed and aging inside this area (measuring about  $200 \text{ cm}^2$ ) may be produced only by ion impact related to Cherenkov photons. At a gain of  $10^5$  and with an average of 20 photoelectrons per event, up to  $10 \mu\text{C}/\text{cm}^2$  are accumulated inside such a fiducial area during one week of test-beam exposure.

b) *PC29 to PC32* - Given their larger size, the QE of these PCs was evaluated by means of a test-beam scan in three different fixed locations (for each PC). The local irradiation, inside the  $1 \text{ cm}^2$  beam fiducial area, is much higher than in the Cherenkov fiducial region, leading to a total accumulated charge density of the order of  $1 \text{ mC cm}^{-2}$  (over all the periods of beam tests). Proto-2 was also exposed to fixed-target events at the CERN/SPS (350 GeV/c  $\pi^-$  on Be) and to Au-Au collision or cosmic rays events at STAR, with Cherenkov rings spread over the whole detector surface. For the  $\pi^-$ -Be events, an average multiplicity of 100 particles/ $\text{m}^2$  was measured inside an acceptance region of 5 cm radius, gathering up to  $50 \mu\text{C}/\text{cm}^2$  over the irradiated PC32 and PC31. For the Au-Au events, an average multiplicity of 20 particles/ $\text{m}^2$  was measured in central events, collecting  $20 \mu\text{C}/\text{cm}^2$  over the whole photosensitive area.

##### iii) Photon impact.

The largest photon flux of  $2 \times 10^4 \text{ photons cm}^{-2} \text{ s}^{-1}$ , estimated inside the Cherenkov fiducial area, was reached with the beam in fixed positions. This value is very far from the flux of  $10^{12} \text{ cm}^{-2} \text{ s}^{-1}$  necessary to observe aging due to photon impact only. Results of this effect can be found in [3,4,12,13].

## 5. Selected PCs history and stability

Fig. 5 shows the evolution with time of the mean QE over the wavelength range 155-210 nm as a function of PC age for PC19 and PC24.

PC19 underwent three mountings on a detector without a glove-box, resulting in a QE decay of about 20%. However, in the following tests a remarkably constant performance was observed, up to a total accumulated charge density of  $50 \mu\text{C}/\text{cm}^2$ .

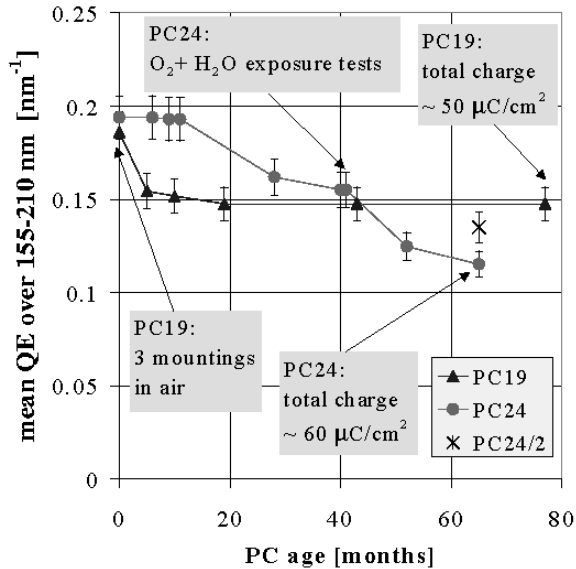


Fig. 5 Mean QE history of PC19 and PC24. The point labeled as PC24/2 refers to a different fiducial area than the usual one, obtained by reducing the proximity gap in proto-1. Each point in the plot corresponds to an irradiation period of about one week at the test-beam.

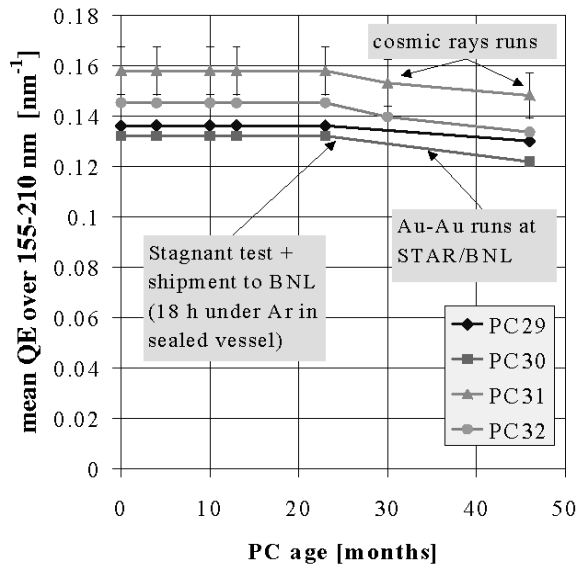


Fig. 6 Mean QE history of the proto-2 PCs (PC29 to PC32). Each point in the plot corresponds to an irradiation period of about one week at the test-beam or with cosmic rays.

PC24 began to deteriorate after initial stability, for reasons that are not yet clear. One possible origin could be a leak from the radiator causing an accidental exposure to air and  $\text{C}_6\text{F}_{14}$ . Additionally, given the technology to produce the pad PCB for PC24, the presence of micro-leaks (caused by through-holes for pad-electronics connection) cannot be excluded. Afterwards, two kinds of exposure tests were performed: (1) 24 h stagnant test, outgassing 10000 ppm of  $\text{O}_2$  and 40 ppm of  $\text{H}_2\text{O}$ ; (2) under Ar/dry air mixture flow, 6 and 18 h with 18000 ppm of  $\text{O}_2$  and 6 h with 100000 ppm of  $\text{O}_2$ . Soon after each of these tests, no degradations were observed. However, later checks have pointed out a worsening of the QE, with about the same aging slope. In the last test-beam, a different fiducial area was investigated, resulting in a slightly larger QE (star symbol in Fig.5). Considering that such a fiducial area was never irradiated, this result seems to confirm what we found for PC19, namely that the exposure to pollutants is the main reason of the CsI QE degradation, at least for the considered accumulated charge.

Fig. 6 shows the variation with time of the mean QE of the proto-2 PCs (PC29 to PC32). The four PCs have shown very high stability up to a total collected charge density (over the whole detector photosensitive area) of  $80 \mu\text{C}/\text{cm}^2$ . Before the shipment to BNL, the HMPID proto-2 was kept for 16 h without gas flow, with an overpressure of 3 mbar, reaching 5000 ppm of  $\text{O}_2$  and 30 ppm of  $\text{H}_2\text{O}$  due to the outgassing. Even in this case, no variations of the QE were detected soon after the test. However, this test and the shipment to BNL (18 h in a sealed container) might have initiated the small QE decrease (less than 10%), measured with two cosmic rays test periods.

However, about two years of operation at STAR have not affected the four PCs performance. In addition, the STAR and the cosmic rays runs have allowed to assess the response of PCs inside the fixed beam fiducial areas, where up to  $\sim 1 \text{ mC cm}^{-2}$  have been collected during the test-beam periods. Indeed, Fig.7 shows the proto-2 pad map with 30000

overlapped STAR events. No dead or lower efficiency regions have been observed in such beam fixed locations, centered at the following pad coordinates:  $Y=24$  and  $72$ ,  $X=20$ ,  $40$ ,  $60$ ,  $80$ ,  $100$ , and  $120$ . For comparison, the charge density integrated over a one year ( $10^6$  s) Pb run at ALICE (with 3% central events) is expected to amount to  $50 \mu\text{C}/\text{cm}^2$ .

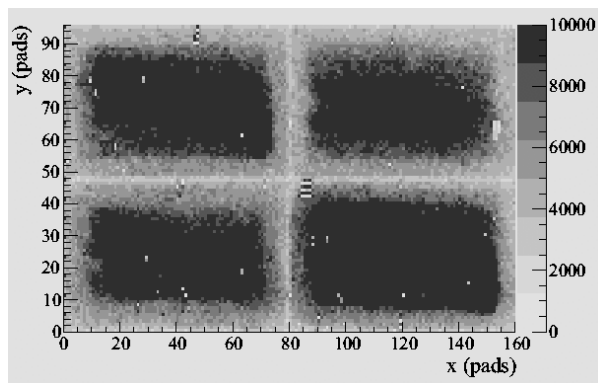


Fig. 7 Pad map of proto-2 obtained by overlapping 30000 STAR events. Only the hits originated by Cherenkov photons have been considered. The grey scale is proportional to the number of hits in each pad. The lower hit density close to the contour of the PCs is determined by the detector acceptance geometry, while the white spots are dead channels.

## 6. Experience with neutral particles

In 1995-96, more relevant information was obtained from the operation, during two periods of four weeks, of a CsI-based imaging detector in the NA44 experiment, using a Pb beam on target at the CERN/SPS. PC21 and PC22 ( $20 \times 77 \text{ cm}^2$ ) were installed in the photodetectors, as part of the Threshold Imaging Cherenkov detector (TIC) [14]. It was located close to the beam dump and high currents (100-400 nA) were measured at each beam spill. However, the magnetic spectrometer in use at NA44 was designed such that very few charged particles were traversing the gaseous radiator of the TIC, without even crossing the photodetectors. Hence, a large part of the current could have been produced by neutron conversions. During these

periods, the performance of the PCs was found to be stable and the detector operation to be satisfactory.

## 7. Conclusions

The long-term operational experience with 6 large area CsI PCs, produced for the ALICE HMPID prototypes, has been reviewed with respect to the main known aging sources: exposure to air and ion impact.

In PC19, a QE degradation of 20% was observed after exposure to air for about 1 h at a relative humidity of 50%. The contact with high levels (larger than 1000 ppm) of  $\text{O}_2$  does not seem to be harmful, since no remarkable effects have been observed in PC24 and in PC29 to PC32.

Irradiation at rates  $\sim 100 \text{ KHz}$ , leading to local accumulated charge densities of up to  $1 \text{ mC cm}^{-2}$ , has produced neither variations of the CsI QE nor detector performance instabilities. The PC response has been found to be very stable, provided the exposure to  $\text{O}_2$  and  $\text{H}_2\text{O}$  is limited to the ppm level.

## Acknowledgements

The results presented in this paper summarize several years of tests that could not have been accomplished without the invaluable work and technical support of T. D. Williams.

## References

- [1] ALICE collaboration, Technical Proposal, CERN/LHCC 95/71.
- [2] ALICE HMPID Technical Design Report, CERN/LHCC 98-19.
- [3] A. Breskin, Nucl. Instr. and Meth. A 371 (1996) 116.
- [4] J. Va'vra, Nucl. Instr. and Meth. A 387 (1997) 137, and J. Va'vra, et al., Nucl. Instr. and Meth. A 387 (1997) 154.
- [5] V. Peskov, these proceedings.
- [6] <http://www.webelements.com>.
- [7] F. Piuz, et al., Nucl. Instr. and Meth. A 433 (1999) 222.
- [8] RD26 status reports: CERN/DRDC 93-96, CERN/DRDC 94-49, CERN/DRDC 96-20.
- [9] J. Almeida, et al., Nucl. Instr. and Meth. A 367 (1995) 332.
- [10] A. Di Mauro, et al., Nucl. Instr. and Meth. A 433 (1999) 190.
- [11] A. Di Mauro, et al., Nucl. Instr. and Meth. A 461(2001) 584.

[12] P. Krizan, et al., Preprint IJS-DP-7087 (1994).

[14] C. W. Fabjan, et al., Nucl. Instr. and Meth. A 367 (1995) 24.

[13] P. Krizan, et al., Nucl. Instr. and Meth. A 367 (1995) 257.